RI 9402

REPORT OF INVESTIGATIONS/1992



# Materials of Construction for High-Salinity Geothermal Brines

By John P. Carter and Stephen D. Cramer

UNITED STATES DEPARTMENT OF THE INTERIOR

BUREAU OF MINES

**Mission:** As the Nation's principal conservation agency, the Department of the Interior has responsibility for most of our nationally-owned public lands and natural and cultural resources. This includes fostering wise use of our land and water resources, protecting our fish and wildlife, preserving the environmental and cultural values of our national parks and historical places, and providing for the enjoyment of life through outdoor recreation. The Department assesses our energy and mineral resources and works to assure that their development is in the best interests of all our people. The Department also promotes the goals of the Take Pride in America campaign by encouraging stewardship and citizen responsibility for the public lands and promoting citizen participation in their care. The Department also has a major responsibility for American Indian reservation communities and for people who live in Island Territories under U.S. Administration.

Report of Investigations 9402

# Materials of Construction for High-Salinity Geothermal Brines

By John P. Carter and Stephen D. Cramer

UNITED STATES DEPARTMENT OF THE INTERIOR
Manuel Lujan, Jr., Secretary

BUREAU OF MINES
T S Ary, Director

**Library of Congress Cataloging in Publication Data:**

**Carter, J. P. (John P.)**

Materials of construction for high-salinity geothermal brines / by John P. Carter and Stephen D. Cramer.

p. cm. — (Report of investigations / U.S. Dept. of the Interior, Bureau of Mines; 9402)

Includes bibliographical references (p. 8).

Supt. of Docs. no.: I 28.23:9402.

1. Geothermal engineering—California—High-salinity brines—Equipment and supplies—Corrosion. 2. Geothermal brines—California—Salton Sea. 3. Corrosion and anti-corrosives. I. Cramer, Stephen D. II. Title. III. Series: Report of investigations (United States. Bureau of Mines); 9402.

TN23.U43 [TJ280.7] [621.1'623—dc20] 91-25177 CIP

# CONTENTS



## ILLUSTRATIONS



## TABLES

## UNIT OF MEASURE ABBREVIATIONS USED IN THIS REPORT

| | | | |
|---|---|---|---|
| °C | degree Celsius | μm/yr | micrometer per year |
| h | hour | mV | millivolt |
| kcal/mol | kilocalorie per mole | ppm | part per million |
| kW-h | kilowatt hour | V | volt |
| L/min | liter per minute | V/h | volt per hour |
| μm | micrometer | wt pct | weight percent |

# MATERIALS OF CONSTRUCTION FOR HIGH-SALINITY GEOTHERMAL BRINES

By John P. Carter[1] and Stephen D. Cramer[2]

## ABSTRACT

The U.S. Bureau of Mines conducted research to determine suitable construction materials for use in brine and steam environments produced from high-salinity geothermal brines. The high-temperature, high-salinity geothermal brines in the Salton Sea Known Geothermal Resources Area (KGRA) are a valuable source of energy and mineral values. The brine and steam produced from them are corrosive and cause early failure of many common materials of construction. Mass-loss and electrochemical corrosion measurements were conducted on over 60 metal alloys in brine and steam environments produced from geothermal well Magmamax No. 1, located at the Salton Sea KGRA, at temperatures from 180° to 215° C, and in synthetic Magmamax brine at 105° and 232° C. General corrosion, crevice and pitting corrosion, and stress corrosion were examined along with the effects of dissolved gases. The alloys with the most acceptable corrosion performance in high-temperature, high-salinity geothermal environments were the high-chromium ferritic stainless steels, the Inconels and Hastelloys, and the titanium alloys. Specific alloys that performed well in wellhead brine included Fe29Cr4Mo, E-Brite 26-1, stabilized Fe26Cr1Mo, 6X, Inconel 625, Hastelloy C-276, Hastelloy S, Hastelloy G, Ti50A, Ti0.2Pd, and TiCode 12.

[1]Corrosion engineer, M&DP Assoc., Hyattsville, MD.
[2]Chemical engineer, Albany Research Center, U.S. Bureau of Mines, Albany, OR.

## INTRODUCTION

Development of the geothermal resources of the United States could result in the production of $6 \times 10^{12}$ kW-h of electrical energy (*1*).[3] The geothermal fields in the Imperial Valley of California have brines that also contain large quantities of dissolved solids. This is particularly true for the Salton Sea KGRA where total dissolved solids range between 25 and 30 wt pct. Corrosion seriously degrades the performance of construction materials in these brines and impedes development of the fields for the extraction of mineral and energy values.

U.S. Bureau of Mines corrosion research in Salton Sea geothermal brines was conducted to conserve critical and strategic materials through improved materials performance and to extend the service life of process equipment in mining and minerals processing operations. These brines were produced at temperatures up to 250° C and contained dissolved gases such as carbon dioxide, hydrogen sulfide, and methane. They were a unique source of certain mineral values (*2*). The results of field and laboratory corrosion studies conducted in brine and steam process environments produced from liquid-dominated brine from geothermal well Magmamax No. 1 at the Salton Sea KGRA are reported here. Measurements were made on carbon and alloy steels (<12 wt pct Cr) (*3-5*), stainless steels (*4-5*), aluminum (*5-6*), nickel (*4-5, 7*), copper (*4-6*), and titanium alloys (*4-6*), molybdenum (*4-6*), and niobium (columbium) (*6*). Critical data on the performance of these alloys are summarized here, and new data for the stainless steels are reported.

## EXPERIMENTAL PROCEDURES

Field corrosion studies were conducted in wellhead brine from geothermal well Magmamax No. 1 and in two brine and two steam process environments produced by flash evaporation of the wellhead brine at a test facility on the Salton Sea KGRA in the Imperial Valley, CA (*4*). Over a 7-month period, when the well was producing from 560 to 1,890 L/min, the wellhead brine contained from 96,000 to 130,000 ppm $Cl^-$ and from 167,000 to 214,000 ppm total dissolved solids (*8*). The conditions in the five process environments are given in table 1. Temperatures ranged from 180° to 215° C. The brine environments contained from 115,000 to 129,000 ppm $Cl^-$ and had a pH of 5.3 to 5.8. The steam environments contained from 1,700 to 8,100 ppm $Cl^-$ and had a pH of 6.2 to 6.9 (*3*).

**Table 1.—Conditions in process environments produced using wellhead brine from Magmamax No. 1[1]**

| Process environment | Temp., °C | Absolute pressure, MPa | pH[2] | [$Cl^-$], ppm |
|---|---|---|---|---|
| Wellhead brine . . . . . | 215 | 2.00 | 5.3 | 115,000 |
| Brine from separator 1 . . . | 199 | 1.63 | 5.7 | 127,000 |
| Steam from separator 1 . . | 199 | 1.63 | 6.2 | 8,100 |
| Brine from separator 2 . . . | 180 | 1.02 | 5.8 | 129,000 |
| Steam from separator 2 . . | 180 | 1.02 | 6.9 | 1,700 |

[1]Wellhead brine flow rate was 130 L/min.
[2]Measured at 25° C.

Mass-loss corrosion tests were conducted in the brine and steam environments for periods up to 45 days (*3, 6-8*). Mass-loss samples were used in the as-received condition. Corrosion product and scale were removed from exposed samples by careful scraping and by acid dissolution.

Potentiodynamic and linear polarization electrochemical measurements were made in wellhead brine with the Petrolite M-511E[4] industrial probe (*3, 6-7*). The three-electrode polarization technique was used with a freely corroding electrode of the test material serving as a reference electrode. Potentiodynamic scans were run at 60 V/h, beginning 0.5 V cathodic to the corrosion potential, scanning in the anodic direction, and reversing scan direction in the transpassive region. Polarization resistance was measured using the three-point method (*3, 6-7, 9-10*). All measurements were completed within 0.5 h of immersion of the electrode assembly in fresh brine to minimize the effects of scale deposition on the measurements.

Laboratory mass-loss measurements were conducted in deaerated synthetic Magmamax No. 1 wellhead brine at 105° C in glass reactors and at 232° C in autoclaves for 15 days (*4-5*). Measurements were also made at 232° C in brine containing either 100 ppm $O_2$, 100 ppm $CH_4$, or 250 ppm $CO_2$ (*5, 11-13*).

The metals evaluated in the field and laboratory tests using mass-loss and electrochemical measurements are as shown on the following page. The compositions of the stainless steels are given in table 2. Compositions for the carbon and alloy steels (*3*), nickel alloys (*7*), and copper, titanium, and aluminum alloys (*6*), niobium and molybdenum (*6*) are given elsewhere.

[3]Italic numbers in parentheses refer to items in the list of references at the end of this report.

[4]Reference to specific products does not imply endorsement by the U.S. Bureau of Mines.

*Carbon and alloy steels (<12 wt pct Cr):*

| | |
|---|---|
| Carbon steel | 4130 |
| Fe0.1Cr | Cor-Ten A |
| Cor-Ten B | Mariner |
| Fe1Cr | Fe2.25Cr1Mo |
| Fe5Cr | Croloy 5 |
| Croloy 7 | Croloy 9M |
| Fe9Cr1Mo | Fe10Cr |

*Stainless steels (>12 wt pct Cr):*

| | |
|---|---|
| 410 | 430 |
| 304 | 316L |
| Fe12Cr | Fe18Cr |
| 6X | Sandvik 3RE60 |
| E-Brite 26-1 | Carp 20Cb3 |
| Fe18Cr2Mo | Ex58 |
| Intermediate ferritic | Fe28Cr |
| 26-1s | Fe29Cr4Mo |
| Fe29Cr4Mo2Ni | |

*Nickel alloys:*

| | |
|---|---|
| Nickel 201 | Monel 400 |
| Monel 404 | Incoloy 800 |
| Incoloy 825 | Inconel 600 |
| Inconel 625 | Inconel x-750 |
| Hastelloy C-276 | Hastelloy G |
| Hastelloy S | Pyromet 31 |
| Berylco 440 | |

*Other alloys:*

| | |
|---|---|
| Naval brass | Berylco 50 |
| Berylco 717 | 70-30 CuNi |
| 90-10 CuNi | Ti50A |
| Ti1.5Ni | Ti10V |
| Ti1.7W | Ti0.2Pd |
| Ti6A14V | Ti6Al2Nb1Ta1Mo |
| TiCode 12 | Al 2024-T3 |
| Al 6061-T6 | Mo |
| Nb | |

**Table 2.—Composition of stainless steels,[1] weight percent**

| Alloy | Cr | Mo | Ni | C | Mn | Si | Other |
|---|---|---|---|---|---|---|---|
| Fe12Cr | 11.0 | 0 | 0 | 0.008 | <0.1 | <0.03 | <0.1 Ti, 0.009 N. |
| 410 | 12.5 | 0 | 0 | .14 | .9 | .8 | None. |
| Fe18Cr | 16.2 | 0 | 0 | .007 | <.1 | <.03 | <0.1 Ti, 0.011 N. |
| 430 | 17.0 | 0 | 0 | .1 | .38 | .71 | 0.22 Cu, 0.02 Ti, 0.05 Al. |
| 316L | 17.0 | 2.3 | 12.0 | .004 | 1.74 | .68 | None. |
| Fe18Cr2Mo | 18.5 | 1.4 | .1 | .025[2] | .06 | ND | 0.8[2](Ti+Nb), 0.035[2] N. |
| 304 | 18.5 | 0 | 8.5 | .07 | 1.6 | .9 | None. |
| 6X | 20.0 | 6.3 | 26.0 | .03 | 1.5 | .5 | Do. |
| Carpenter 20Cb3 | 20.0 | 2.3 | 34.0 | ND | ND | ND | 0.5 Nb, 3.2 Cu. |
| Ex58 | 20.5 | 5.0 | 15.4 | .07 | 5.4 | .27 | 0.26 N. |
| Intermediate ferritic | 25.0 | 3.5 | 2.0 | ND | ND | ND | 0.25 Nb, 0.10 Ti. |
| Fe28Cr | 25.4 | 0 | 0 | .010 | <.1 | <.1 | <0.1 Ti, 0.015 N. |
| E-Brite 26-1[3] | 25.7 | 1.0 | .1 | .010 | .3 | .26 | 0.08 Nb, 0.002 Ti, 0.009 N. |
| 26-1 | 26.0 | 1.0 | ND | .002 | ND | ND | 0.010 N. |
| 26-1s[4] | 26.1 | 0.9-1.1 | .2 | .020 | .25 | .22 | 0.02 Nb, 0.68 Ti, 0.010 N. |
| Fe29Cr4Mo | 28.9 | 4.0 | .1 | .004 | .08 | .09 | 0.004 N. |
| Fe29Cr4Mo2Ni | 29.5 | 3.8 | 2.1 | .004 | .07 | .03 | 0.020 N. |

ND Not determined.
[1]Balance iron.
[2]Maximum.
[3]Electron beam melted.
[4]Argon-oxygen decarburized.

## RESULTS AND DISCUSSION

Scale, which readily forms in the high-salinity brine, can constrict flow through process equipment and pipelines. Scale from wellhead brine was mainly silica and galena. It was primarily calcium carbonate from the low-temperature (180° C) separated brine and steam. Scale is periodically removed from pipelines by pigging or using chemical methods (*14*). These operations can increase the corrosion rate substantially by removing semiprotective scale and corrosion product.

The following results and discussion apply to the five process environments in the field studies and to deaerated brine in the laboratory studies. The effect of added gases will be discussed later.

## FERROUS ALLOYS

### Carbon and Alloy Steels (< 12 wt pct Cr)

General corrosion rates for 1020 carbon steel, Mariner, Cor-Ten A, and 4130 steel ranged from 90 to 2,400 μm/yr in the brine environments (*3*). General corrosion rates in the steam environments ranged from 120 to 990 μm/yr. The alloy steels corroded at substantially lower rates than carbon steel. Corrosion rates decreased substantially with time in all the environments, indicating that most corrosion occurred within the first 15 to 30 days of exposure and that the scale and corrosion product offered some protection.

Average pit depths for 1020 carbon steel, Mariner, Cor-Ten A, and 4130 steel ranged from 150 to 400 μm in 15-day exposures in the brine environments. Average pit depths in the steam environments ranged from 140 to 330 μm. Maximum pit depths were two to three times greater than average pit depths. Maximum and average pit depths did not change significantly with exposure time; pit propagation was largely completed within 15 days. In 4130 steel, the deepest pits were formed in the heat-affected-zone of welds. Crevice corrosion occurred to all the steels in each of the environments.

Potentiodynamic polarization measurements in wellhead brine indicated that passive films would form on steels containing more than 1 wt pct Cr. Passive region width broadened with increasing chromium concentration and the addition of molybdenum. Molybdenum additions to the steels shifted the protection potential ($E_{prot}$) from the active region into the passive region.

The general corrosion rate of the steels in wellhead brine, measured by linear polarization, decreased by a factor of 3 with the addition of 3 to 5 wt pct Cr to carbon steel. Further increases in chromium concentration did not reduce the corrosion rate. Additions of molybdenum, nickel, and copper did not affect the corrosion rate of the steels.

### Stainless Steels (> 12 wt pct Cr)

General corrosion rates for selected stainless steels in brine and steam environments, based on four 15-day exposures, are given in table 3. Total corrosion, reported as surface recession, was essentially the same in exposures of 15, 30, and 45 days, indicating that the scale and corrosion product protected the metal from further corrosion within this period. Table 3 reports the surface recession (in micrometers) that occurred after 45 days of exposure. General corrosion rates for 410 stainless steel in brine environments were 20 times greater than rates for Fe29Cr4Mo. In steam environments, 410 stainless steel corroded 50 times greater than Fe29Cr4Mo. Corrosion rates for Fe29Cr4Mo were 28 μm/yr in wellhead brine and 5 μm/yr or less in the other environments. These results translate into a surface recession of 1.1 μm or less for each of the environments after 45 days of exposure. The general corrosion resistance of the stainless steels increased with chromium and molybdenum content; nickel had no significant effect.

**Table 3.—General corrosion of stainless steels in brine and steam environments**

| Alloy | Corrosion rate,[1] μm/yr | Surface recession in 45 days exposure, μm |
|---|---|---|
| BRINE ENVIRONMENTS | | |
| Wellhead brine: | | |
| 410 | 600 | 34.4 |
| 430 | 305 | 23.4 |
| 316L | 411 | 16.9 |
| 6X | 127 | 5.2 |
| Carpenter 20Cb3 | ([2]) | 4.1 |
| E-Brite 26-1 | 107 | 4.4 |
| Fe29Cr4Mo | 27.9 | 1.1 |
| Brine from separator 1: | | |
| 410 | 196 | 17.3 |
| 430 | 25.4 | 5.6 |
| 316L | 94 | 3.9 |
| 6X | 15.2 | .6 |
| Carpenter 20Cb3 | ([2]) | ([2]) |
| E-Brite 26-1 | 17.8 | 1.2 |
| Fe29Cr4Mo | 5.1 | .3 |
| Brine from separator 2: | | |
| 410 | 142 | 20.9 |
| 430 | 12.7 | .6 |
| 316L | 12.7 | .5 |
| 6X | 0 | 0 |
| Carpenter 20Cb3 | ([2]) | ([2]) |
| E-Brite 26-1 | 7.6 | .3 |
| Fe29Cr4Mo | 5.1 | .2 |
| STEAM ENVIRONMENTS | | |
| Steam from separator 1: | | |
| 410 | 279 | 19.4 |
| 430 | 88.9 | 8.8 |
| 316L | 53.3 | 5.9 |
| 6X | 30.5 | 1.9 |
| Carpenter 20Cb3 | 45.7 | ([2]) |
| E-Brite 26-1 | 22.9 | 2.5 |
| Fe29Cr4Mo | 5.1 | .9 |
| Steam from separator 2: | | |
| 410 | 145 | 4.7 |
| 430 | 10.2 | .6 |
| 316L | 25.4 | 4.4 |
| 6X | 0 | 0 |
| Carpenter 20Cb3 | ([2]) | .3 |
| E-Brite 26-1 | 5.1 | .6 |
| Fe29Cr4Mo | 2.5 | .3 |

[1]Average of results from four 15-day exposures.
[2]No samples were exposed.

The maximum and average depth of pits formed in brine and steam environments after 45 days exposure are

given in table 4. Average pit depths for 410 stainless steel were a factor of 2 to 3 times greater than depths for Fe29Cr4Mo in each environment. Average pit depths for Fe29Cr4Mo were 100 μm or less and did not vary with time. Molybdenum improved the resistance of the stainless steels to pitting corrosion in all environments; chromium and nickel had no significant effect. In fact, pit depths for 400-series stainless steels in wellhead brine were similar to those for alloy steels.

**Table 4.—Maximum and average pit depths in 45-day exposures for stainless steels in brine and steam environments, μm**

| Alloy | Maximum | Average[1] |
|---|---|---|
| BRINE ENVIRONMENTS | | |
| Wellhead brine: | | |
| 410 | 668 | 330 |
| 430 | 534 | 298 |
| 316L | 332 | 196 |
| 6X | 510 | 82 |
| Carpenter 20Cb3 | 256 | 198 |
| E-Brite 26-1 | 711 | 266 |
| Fe29Cr4Mo | 489 | 96 |
| Brine from separator 1: | | |
| 410 | 310 | 158 |
| 430 | 282 | 141 |
| 316L | 335 | 113 |
| 6X | 140 | 42 |
| Carpenter 20Cb3 | 190 | 140 |
| E-Brite 26-1 | 316 | 106 |
| Fe29Cr4Mo | 256 | 80 |
| Brine from separator 2: | | |
| 410 | 289 | 125 |
| 430 | 224 | 107 |
| 316L | 207 | 100 |
| 6X | 106 | 36 |
| Carpenter 20Cb3 | ([2]) | ([2]) |
| E-Brite 26-1 | 427 | 84 |
| Fe29Cr4Mo | 179 | 56 |
| STEAM ENVIRONMENTS | | |
| Steam from separator 1: | | |
| 410 | 363 | 169 |
| 430 | 279 | 165 |
| 316L | 302 | 125 |
| 6X | 154 | 45 |
| Carpenter 20Cb3 | 275 | 182 |
| E-Brite 26-1 | 549 | 109 |
| Fe29Cr4Mo | 197 | 66 |
| Steam from separator 2: | | |
| 410 | 207 | 125 |
| 430 | 271 | 94 |
| 316L | 194 | 82 |
| 6X | 211 | 92 |
| Carpenter 20Cb3 | 242 | 123 |
| E-Brite 26-1 | 515 | 88 |
| Fe29Cr4Mo | 96 | 52 |

[1]Average of results from four 15-day, one 30-day, and one 45-day exposure.
[2]No samples were exposed.

Type 316L stainless steel exhibited transgranular stress corrosion cracking in all the environments (*4*, *15*). Type 410 and 430 stainless steels exhibited crevice corrosion in all the environments (*4-5*). Type 316L, Carpenter 20Cb3, 6X, E-Brite 26-1, and Fe29Cr4Mo were most susceptible to crevice corrosion in wellhead brine and steam environments. The heat-affected-zone of butt-welded Fe29Cr4Mo exhibited weld decay in wellhead brine.

Potentiodynamic scans for stainless steels in wellhead brine are plotted in figure 1 with the logarithm of the current density, j, as one axis and the potential of the alloy compared with a freely corroding electrode of the same alloy (reference electrode) the other axis. All the scans have the same horizontal scale, are referenced to the corrosion potential of the steel, and are shifted vertically to separate the curves. $E_A$ is the activation or Flade potential; $E_B$ is the breakdown potential. All the stainless steels exhibited an active-passive transition. Molybdenum additions broadened the passive region ($E_B$-$E_A$), shifted the protection potential ($E_{prot}$) into the passive region, and expanded the region ($E_{prot}$-$E_A$) where steel is immune to pitting. Pits tend to propagate but do not initiate in the region ($E_B$-$E_{prot}$). This region is plotted in figure 2 versus the passive region width. The FeCr alloys lie on the diagonal line, indicating that pits once initiated are unlikely to repassivate in this material. The FeCr(Mo,Ni) alloys lie below this line, and conditions exist where repassivation of pits in this material can occur. This is due to the broadening of the passive region by molybdenum and helps explain the beneficial effect of molybdenum on pitting and general corrosion.

General corrosion rates of 15 stainless steels in wellhead brine, measured by linear polarization, spanned a 30-fold range. These rates were higher than those measured by mass loss because the steels were in a "scale-free" condition for the polarization measurements. There may also be differences because of the values assumed for the Tafel constants in the equation used to compute the corrosion current. Fe29Cr4Mo had the lowest rate, 77 ±38 μm/yr. The rates for the stainless steels (and those for carbon steel and alloy steels) are given in figure 3 showing the effect of alloy composition on corrosion rate. The FeCr alloys are represented by the solid curve. Molybdenum and nickel had no effect on the corrosion rate below 12 wt pct Cr. Above 12 wt pct Cr, molybdenum, and nickel had a beneficial effect, which can result in an order of magnitude decrease in the general corrosion rate. The striped area in figure 3 is the region of enhanced corrosion resistance resulting from alloy additions to the basic FeCr alloy. Several alloys, including the ferritic stainless steels Fe29Cr4Mo and Fe29Cr4Mo2Ni, lie within this region and had excellent resistance to crevice corrosion, pitting corrosion, and stress-corrosion cracking.

Activation energies, based on 15-day general corrosion rates at temperatures from 180° to 215° C, were the same in brine and steam environments, i.e., 15.8 kcal/mol. The

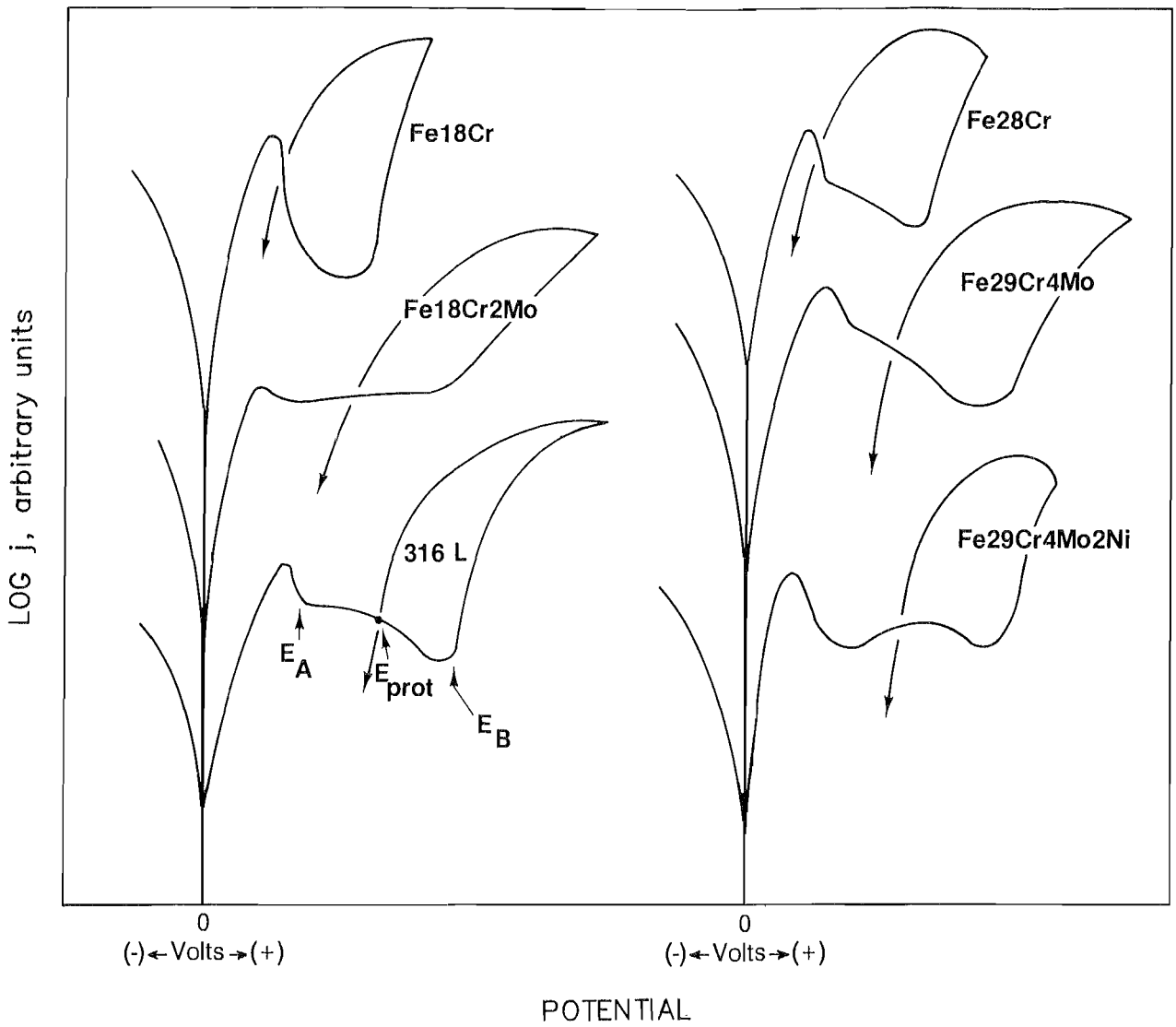


**Figure 1.—Potentiodynamic polarization scans for stainless steels in wellhead brine from Magmamax No. 1 at 215°C. Scan rate = 60 V/h. (Scans shifted vertically for purposes of illustration; same horizontal scale used for each scan.)**

corresponding value for pitting corrosion was 5.1 kcal/mol, indicating that pitting corrosion was less sensitive to temperature than was general corrosion.

## NICKEL ALLOYS

General corrosion rates for Monel 400, Monel 404, Inconel 600, Inconel 625, Incoloy 825, Hastelloy G, and Hastelloy S ranged from 0 to 720 μm/yr in the brine environments in 15-day exposures (*7*). Rates in the steam environments ranged from 0 to 400 μm/yr. Nickel 201 corroded at rates about twice those of the other nickel alloys. Monel 404 corroded more rapidly than Monel 400 in all but the wellhead brine. Chromium additions of 15 wt pct substantially lowered the corrosion rate of the nickel alloys. Except for Incoloy 825, which corroded at 120 μm/yr in wellhead brine, Incoloy 825, Inconel 625, Hastelloy G, and Hastelloy S corroded at rates less than 25 μm/yr in all environments. Protective scale formation greatly reduced corrosion after the first 15 days of exposure.

Average pit depths for Monel 400, Monel 404, Inconel 600, Inconel 625, Incoloy 825, Hastelloy G, and Hastelloy S spanned a threefold range and were under 100 μm in each environment. The deepest pits were in Hastelloy G and Incoloy 825 in brine and in Incoloy 825 in steam. Few pits were observed in Monel 400, Monel 404, and Hastelloy S in wellhead brine, or in Hastelloy S, Hastelloy G, and

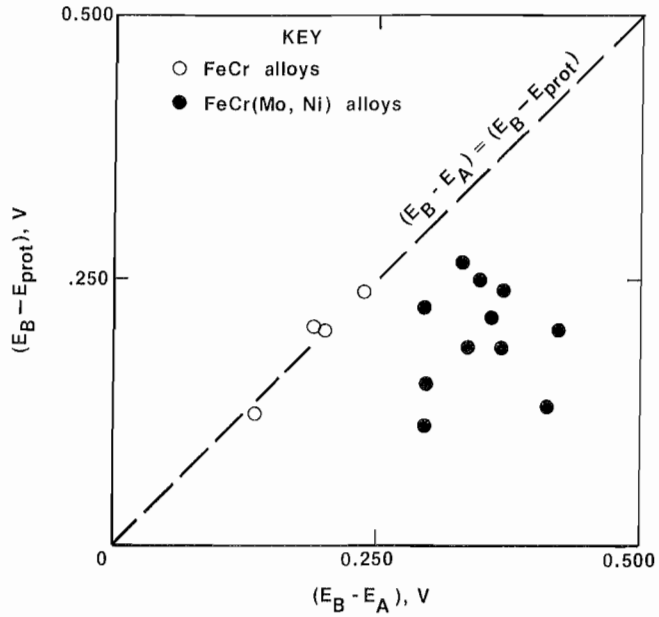


**Figure 2.—Comparison of passive region width to potential range over which pits propagate in wellhead brine from Magmamax No. 1 at 215° C.**

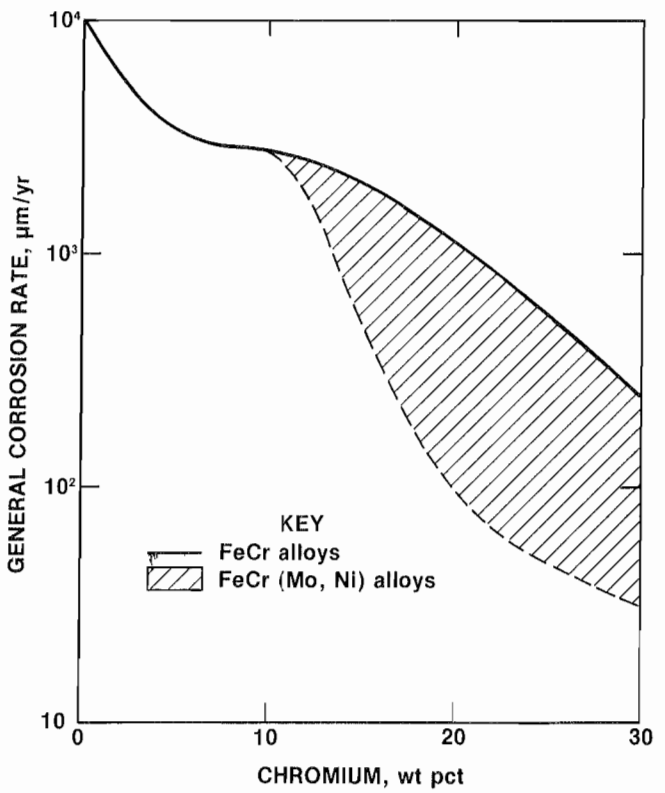


**Figure 3.—Corrosion rate of FeCr and FeCr(Mo,Ni) alloys in "scale-free" condition in wellhead brine from Magmamax No. 1 at 215° C measured by linear polarization.**

Inconel 625 in steam. Pitting occurred largely in the first 15 days of exposure (*7*).

No stress-corrosion cracking occurred in Monel 400, Monel 404, Inconel 600, Inconel 625, Hastelloy S, and Hastelloy G. Incoloy 825 cracked in wellhead brine. Monel 400 and Monel 404 exhibited severe nonuniform corrosion in wellhead brine. Incoloy 825 exhibited crevice corrosion in brine and in one steam environment. Except for Incoloy 825, the nickel alloys did not exhibit crevice corrosion in steam.

Based on potentiodynamic scans, all the nickel alloys exhibited active-passive behavior in wellhead brine. The passive region was broadest for NiCr alloys containing high levels of molybdenum, such as Inconel 625 and Hastelloy C-276. For Nickel 201, Monel 400 and Berylco 440, the protection and breakdown potentials were equivalent. These alloys are unlikely to pit while the surface is passive. Inconel 625 and Hastelloy C-276 were not entirely immune to pitting corrosion in the passive region (*7*).

The general corrosion rates of nine nickel alloys in wellhead brine, measured by linear polarization, spanned a 10-fold range. The lowest corrosion rate observed was for Hastelloy C-276, 81 ±25 µm/yr. This result underscores the strong beneficial effect of chromium and molybdenum on the corrosion performance of the nickel alloys (*7*).

## OTHER ALLOYS

The titanium alloys were highly resistant to general corrosion in brine and steam environments (*4-6*). TiCode 12 did not corrode in these environments. Measurable corrosion was observed in wellhead brine only for Ti50A and Ti6Al4V; the corrosion rates were 30 and 100 µm/yr, respectively. Ti6Al4V was susceptible to pitting in brine environments. None of the titanium alloys pitted in steam. Titanium 50A, TiCode 12, and Ti6Al4V showed evidence of mild crevice corrosion in some environments. Stress-corrosion cracking of the titanium alloys was not observed in exposures of 45 days in brine or steam. The titanium alloys exhibited passive behavior over a potential range of more than 1 V during potentiodynamic scans in wellhead brine. No evidence of susceptibility to pitting corrosion in the passive region was observed for Ti50A and Ti6Al2Cb1Ta1Mo. General corrosion rates measured by linear polarization in wellhead brine ranged from 8 ±0.3 µm/yr for Ti6Al2Cb1Ta1Mo to 27 ±0.7 µm/yr for Ti50A.

The copper alloys exhibited active-passive behavior during potentiodynamic polarization measurements in wellhead brine (*6*). Passive regions were broad, between 200 and 300 mV, for 70-30 CuNi and Berylco 717. Naval brass had a narrow passive region, evidently due to its high zinc content. General corrosion rates in wellhead brine, measured by linear polarization, were high and ranged from 1,770 ±350 µm/yr for 70-30 CuNi to 730 ±25 µm/yr for 90-10 CuNi. Iron additions appeared to accelerate corrosion.

Molybdenum and niobium were resistant to general corrosion, and crevice and pitting corrosion in brine and steam environments (*6*). The aluminum alloys 2024-T3 and 6061-T6 corroded rapidly even in low-temperature (105° C) Salton Sea KGRA brine and exhibited severe crevice and pitting corrosion (*5-6*).

### DISSOLVED GAS EFFECTS

Compared with deaerated brine, brine containing 100 ppm $O_2$ greatly increased the general corrosion rate of carbon and alloy steels, stainless steels, and nickel alloys. It did not affect general corrosion of titanium alloys. Stress-corrosion cracking of stainless steels occurred in both deaerated brine and brine containing 100 ppm $O_2$. Dissolved oxygen also produced stress cracking in Inconel 625, Ti50A, and Hastelloy C-276 (*4-5*). Iron and nickel alloys experienced severe crevice corrosion in brine containing 100 ppm $O_2$, but none was observed in titanium alloys. Oxygen produced pitting in Inconel 625 and Hastelloy C-276, but none in Ti50A (*4-5*). Dissolved carbon dioxide and methane had little effect on the corrosion rate of the metals.

## CONCLUSIONS

The corrosive high-temperature, high-salinity brine and steam process environments produced from geothermal brines, such as those from the Salton Sea KGRA, require careful selection of construction materials. Problems associated with crevice corrosion and stress intensity can be addressed in part by engineering design, which expands the range of useful materials. Carbon and alloy steels, copper, and aluminum alloys were unsuitable because of high corrosion rates and severe crevice corrosion and pitting. The Monels and Ni201 were unsuitable because of high corrosion rates. The austenitic stainless steels were unsuitable because they are susceptible to stress corrosion cracking.

The alloys that appeared most suitable for service in these severe environments include the high-chromium ferritic stainless steels, the Inconels and Hastelloys, and the titanium alloys. Specific alloys which performed well in wellhead brine were Fe29Cr4Mo, E-Brite 26-1, stabilized Fe26Cr1Mo, 6X, Inconel 625, Hastelloys C-276, S, and G, Ti0.2Pd, TiCode 12, and Ti50A. Ti6Al4V also appeared acceptable, but its corrosion rate was higher than those of the other titanium alloys.

## REFERENCES


1. Dipippo, R. Geothermal Energy: A Viable Supplementary Energy Source. Ch. in Solving Corrosion and Scaling Problems in Geothermal Systems, ed. by J. Carter. Nat. Assoc. Corros. Eng., 1984, pp. 1-19.

2. Schultze, L. E., and D. J. Bauer. Operation of a Mineral Recovery Unit on Brine From the Salton Sea Known Geothermal Resource Area. BuMines RI 8680, 1982, 12 pp.

3. Cramer, S. D., J. P. Carter, and R. K. Conrad. Corrosion and Scaling of Carbon and Alloy Steels in Salton Sea Geothermal Environments. Ch. in Solving Corrosion and Scaling Problems in Geothermal Systems, ed. by J. Carter. Nat. Assoc. Corros. Eng., 1984, pp. 188-208.

4. Cramer, S. D., and J. P. Carter. Corrosion in Geothermal Brines of the Salton Sea Known Geothermal Resource Area. Ch. in Geothermal Scaling and Corrosion, ed. by L. A. Casper and T. R. Pinchback. ASTM Spec. Tech. Publ. 717, 1980, pp. 113-141.

5. ____. Laboratory Corrosion Studies in Low- and High-Salinity Geobrines of the Imperial Valley, Calif. BuMines RI 8415, 1980, 30 pp.

6. Conrad, R. K., J. P. Carter, and S. D. Cramer. Corrosion of Selected Metals and a High-Temperature Thermoplastic in Hypersaline Geothermal Brine. BuMines RI 8792, 1983, 20 pp.

7. Cramer, S. D., J. P. Carter, and R. K. Conrad. Corrosion and Scaling of Nickel Alloys in Salton Sea Geothermal Environments. Ch. in Solving Corrosion and Scaling Problems in Geothermal Systems, ed. by J. Carter. Nat. Assoc. Corros. Eng., 1984, pp. 215-235.

8. Carter, J. P., F. X. McCawley, S. D. Cramer, and P. B. Needham, Jr. Corrosion Studies in Brines of the Salton Sea Geothermal Field. BuMines RI 8350, 1979, 35 pp.

9. Cramer, S. D. Estimation of the Slope of Polarization Curves in the Vicinity of the Corrosion Potential. J. Electrochem. Soc., v. 126, No. 6, 1979, pp. 891-893.

10. Danielson, M. J. Analysis of Errors in Using the Two Electrode and Three Electrode Polarization Resistance Methods in Measuring Corrosion Rates. Corrosion, v. 36, No. 4, 1980, pp. 174-178.

11. Cramer, S. D. The Solubility of Methane, Carbon Dioxide, and Oxygen in Brines From 0° to 300° C. BuMines RI 8706, 1982, 17 pp.

12. ____. Solubility of Methane in Brines From 0 to 300 C, I&EC Process Des. Dev., v. 23, No. 3, 1984, pp. 533-538.

13. ____. Oxygen Solubility in Brines. I&EC Process Des. Dev., v. 23, No. 3, 1984, pp. 618-620.

14. Lewis, W. E., and D. R. Powell. Prevention of Scale Formation in Systems Handling Highly Saline Geothermal Brines. Ch. in Solving Corrosion and Scaling Problems in Geothermal Systems, ed. by J. Carter. Nat. Assoc. Corros. Eng., 1984, pp. 209-214.

15. Goldberg, A. Comments on the Use of 316L Stainless Steel Cladding at the Geothermal Niland Test Facility. UCID-17113, Univ. CA, Livermore, CA, April 30, 1976, 17 pp.


☆ U.S. GOVERNMENT PRINTING OFFICE: 1992--611-214 INT.BU.OF MINES,PGH.,PA 29502